IEEE Access
Multidisciplinary | Rapid Review | Open Access Journal

IEEE VEHICULAR TECHNOLOGY SOCIETY SECTION

Received 18 November 2022, accepted 13 January 2023, date of publication 20 January 2023, date of current version 25 January 2023.

Digital Object Identifier 10.1109/ACCESS.2023.3238466

RESEARCH ARTICLE

Congestion Control in Autonomous Resource Selection of Cellular-V2X

SAIF SABEEH, (Member, IEEE), AND KRZYSZTOF WESOŁOWSKI, (Life Member, IEEE)
Institute of Radiocommunications, Poznan University of Technology, 60-965 Poznan, Poland

Corresponding author: Saif Sabeeh (saifsadeq1982@gmail.com)

This work was supported by the Poznan University of Technology under Grant 0312/SBAD/8162.

ABSTRACT Intelligent transportation systems have recently become a promising technology for future industry to provide safe, green, and automated driving. In this regard, the Third Generation Partnership Project (3GPP) has proposed to utilize cellular communication to enable direct communication between vehicles with and without cellular infrastructure assistance. 3GPP has introduced the Sensing-Based Semi-Persistent Scheduling (S-SPS) technique when coverage of the cellular system is absent. S-SPS faces resource collision and performance degradation problems when channel load increases in the network. This paper suggests a decentralized congestion control and transmission power control mechanism (TPC-DCC) with an adaptive threshold for the received signal as a combination method to decrease channel load in the network. Furthermore, this work introduces a novel channel load adjustment. The new adjusting algorithm is based on a constant difference between the upper and lower boundaries of channel load at each level to handle channel overload and provide more flexibility using DCC mechanisms. The interactions of the proposed algorithm with S-SPS and the Extended-Estimation Reservation Resource Allocation (E-ERRA) algorithms that the authors previously proposed are investigated. The results indicate that system performance can be substantially improved when the transmission power and reception threshold are adaptively adjusted to the proposed channel load adjustment. The results of E-ERRA with the proposed channel load adjustment method show promising results compared to S-SPS.

INDEX TERMS C-V2X, decentralized congestion control, resource collision, S-SPS, E-ERRA.

I. INTRODUCTION

Intelligent transportation systems and automated vehicles will soon be an essential part of future technologies used every day. For many years, dedicated short-range communications (DSRC) based on the IEEE 802.11p standard have been used as the only solution that supports vehicular communication [1]. 3GPP in Release 14 standardized new advanced LTE features to enable basic safety applications using direct information exchange through the SideLink (SL) communication link. SL communication takes place between vehicles themselves and between vehicles and surrounding nodes, such as roadside units, cellular and road infrastructure, and cellular devices. Vehicle communication can be supported by cellular infrastructure or not [2]. This technology is known as Cellular-Vehicle-to-Everything (C-V2X) or LTE-Vehicle-to-Everything (LTE-V2X) communication. It can function in two modes. Mode 3 operates under the supervision of the cellular infrastructure, whereas Mode 4 works without it. 3GPP in Release 15 [3] improved C-V2X to involve non-safety applications with key performance indicators more demanding than in Release 14. More advanced safety and non-safety applications with unicast, groupcast, and broadcast are standardized in Release 16 [4] using SL in intelligent transportation systems and licensed bands (FR1, FR2). This type of communication is called the New Radio Vehicle-to-Everything (NR V2X) communication.

Generally, in LTE-V2X some modifications of the physical layer have been added to manage the Doppler effect in high mobility scenarios [5]. The number of DeModulation Reference Signals (DMRS) in one subframe is increased from two in Device-to-Device (D2D) (3GPP Release 12) to four in C-V2X communication. The Cooperative Awareness

The associate editor coordinating the review of this manuscript and approving it for publication was Hassan Omar.

Message (CAM) has been suggested by ETSI [6] as a periodic message broadcast to surrounding vehicles. This message contains information about speed, movement direction, type, acceleration, and deceleration. IEEE defines it as a Basic Safety Message (BSM) or a Beacon [7], [8].

The CAM message consists of two parts in adjacent or non-adjacent configuration. In two resource blocks, the first part carries the SideLink Control Information (SCI) to help the receiver decode the second part. The second part contains Transport Blocks (TB) within a variable number of resource blocks. Furthermore, SCI and TB are transmitted using the Physical Side Link Control Channel (PSCCH) and the Physical Side Link Shared Channel (PSSCH), respectively [9].

3GPP proposed Sensing-based Semi-Persistent Scheduling (S-SPS) as a Mode 4 scheduling method with the use of the Single Carrier Frequency Division Multiple Access (SC-FDMA) technique. The authors of this article have previously suggested Estimation and Reservation Resource Allocation (ERRA) and Extended-ERRA algorithms as alternative scheduling methods to reduce resource collisions and complexity in the selection and reselection of radio resources [10], [11].

An increased channel load in the given band in the broadcasting range of a vehicle can cause resource collisions and hidden nodes, especially when the number of broadcasters is greater than the limited number of resources. The restricted number of resources depends on several factors such as the data rate and the amount of data that are related to the number of resource blocks in each subchannel [8], the transmission rate, and the coverage area resulting from the transmission power.

In [12] and [13], Decentralized Congestion Control (DCC) mechanisms are proposed for VANET communication to deal with the increasing channel load issue by adapting the parameters of the physical layer throughout such as transmit power, transmit rate, and data rate. However, the technical standard did not clearly explain the mechanism for selecting the transmit resources for packets when the channel load is high and changes rapidly. Generally, little attention is paid in the literature to investigating interactions between DCC and scheduling methods for C-V2X communication.

The DCC mechanisms consist of three parameter adjusting mechanisms to regulate the channel load as mentioned below. These mechanisms can adjust the transmission power, data rate, or transmission rate based on the Channel Busy Ratio (*CBR*). Furthermore, the DCC mechanism is characterized by three types of states: relaxed, active, and restrictive. In turn, the active state contains one or more active levels that differ in physical parameters. This work proposes an adjusting algorithm to support several levels of *CBR*. A fixed relative difference between the upper and lower boundaries of *CBR* levels provides more flexibility and excellent immunity against high channel overload. The levels of transmission power adaptation using the transmission power mechanism are synchronized with the signal reception sensitivity thresholds to adjust the channel load for the LTE-V2X Mode 4 vehicular communication system. However, the CBR could be understood as the channel utilization. Generally, channel utilization in V2X communication is defined as the ratio of the number of busy subchannels to the total number of subchannels during the broadcast period. The maximum value of channel utilization is usually called channel capacity [14] and [15]. Therefore, 100% channel utilization indicates that there is no free subchannel to transmit data.

This work investigates the interaction of the proposed method with the S-SPS and E-ERRA radio resource scheduling methods in terms of the packet reception ratio and the packet collision ratio. To provide more realistic environments, the simulation has considered two highway scenarios and MCS orders in fixed and varying vehicle densities.

A. RELATED WORKS

A number of research groups have paid attention to the DCC mechanisms applied in C-V2X. One of the first investigations on the DCC mechanisms that enable C-V2X Mode 4 was carried out by Mansouri et al. [16].

Based on the table that contains the fixed number of channel load adjustments that 3GPP proposes, Mansouri investigated the mechanism of dropped packets when the S-SPS scheduling method is applied for LTE-V2X with a fixed number of vehicles.

Furthermore, Mansouri highlighted the S-SPS problem of resource selection when the channel load increases and proposed a packet drop technique to reduce the channel busy ratio. In [17], the authors analyzed the efficiency of the packet drop technique to improve QoS in the application layer and tested the proposed method for several vehicle speeds. Consequently, the authors found that dropping packets as congestion control harms performance at the application layer.

In [19], interactions of DCC mechanisms with the LTE-V2X Mode 4 resource allocation algorithm were investigated by changing the resource reservation interval (RRI) within S-SPS with the measured *CBR* or channel occupancy. Bazzi et al. in [21] recommended further investigations when increasing the frequency of awareness message transmissions without influencing vehicle awareness. Adaptive resource (re)selection with a resource collision detection algorithm was proposed in [22]. In [23], the authors of this article introduced a spectrum partitioning technique to avoid the overlap area of the broadcast in C-V2X Mode 3.

Some studies focus on the comparison between the Cellular-V2X Mode 4 and IEEE 802.11p standards, such as DSRC or ITS-G5 [25], [26], [27], and [28].

The multi-hop clustering algorithm was investigated using a hybrid architecture with infrastructure support [29]. An analytical model for autonomous Cellular-V2X Mode 4 was investigated using the Veins software platform [30] to compare performance at different vehicle densities.

B. PAPER ORGANIZATION

The rest of this paper is organized as follows. The assumptions and general background of C-V2X are presented in Section II. The proposed algorithm applied in S-SPS and E-ERRA is shown in Section III. Section IV presents the system model and simulation scenarios. The system performance and simulation results are described in Section V. Section VI concludes the paper.

II. ASSUMPTIONS AND BACKGROUND

A. CONGESTION CONTROL

In [4], the application of congestion control in LTE-V2X Mode 4 has been specified. The standard does not describe a precise algorithm for controlling channel congestion but presents corresponding metrics and possible mechanisms to decrease the channel load that leads to resource congestion. In each packet (re)transmission, the vehicle has to measure the SL Channel Busy Ratio (CBR) and SL Channel occupancy Ratio (CR). Measurements should be performed in the subframe τ-4 when the transmission of the packet will be broadcast on the subframe τ. CBR indicates the level of channel load, which can be defined as the number of subchannels in the last 100 ms (100 subframes) that feature an average of the Received Signal Strength Indicator (RSSI) higher than a pre-established threshold. On the other hand, CR quantifies the channel occupancy caused by vehicle broadcast packets. It defines the number of subchannels that the vehicle utilizes to transmit during an interval of 1000 ms (1000 subframes). Each vehicle can divide this time period into two intervals, the past and future intervals, and can decide how many past and future subframes for CR are used for measurement. However, the number of past subframes should be equal to or greater than 500. Moreover, only the subframes already used by the broadcasting vehicles can be considered to measure CR. The standard proposed that up to 16 CBR levels can be defined. Vehicles cannot cross CR_{limit}, which increases as the CBR decreases at each level. The value of CR_{limit} is a function of the priority of the TB and the absolute speed of the vehicle. Each vehicle needs to measure CBR and quantifies its CR before the (re)transmission of the packets. If the measured CR is higher than the configured CR_{limit} established for the current level of CBR, the vehicle must reduce this CR to the value below CR_{limit} by adjusting the transmission parameters. However, to achieve this reduction, the standard indicates several potential mechanisms [12]:

- **Transmit power control (TPC):** In TPC, the transmission power changes to adjust to the current channel load. For example, a vehicle decreases its transmission power when a high channel load is observed, reducing the interference range and diminishing the CBR.
- **Transmit rate control (TRC):** This mechanism works by adjusting the time between two consecutive transmission packets sent by a vehicle.
- **Transmit data rate control (TDC):** This mechanism can be used by a vehicle that can transfer data in several rate options. During high channel load time periods and depending on the application, a car can adjust the data rate of the SL transmission to be appropriate for the current channel condition.

It is essential to mention that the standard did not specify the ranges of CBR levels and the weights of CR_{limit} for each level. However, 3GPP introduced a working document considering the ranges of CBR levels. However, our work proposes a new algorithm to assign CBR to each level, compared to the algorithms shown in [16] and [19].

B. C-V2X COMMUNICATION ASSUMPTIONS

As mentioned above, SC-FDMA is applied to periodically broadcast CAM messages in the 10 MHz channel bandwidth. Each subframe consists of two slots (0.5 ms each). In turn, each subchannel consists of a group of Resource Blocks (RB), which are the smallest units allocated within the 180 kHz bandwidth. In each new sub-channel selection, the transmitter generates a random number in a specific range named the Reselection Counter (RC). This number decreases by one in each broadcast, and resource reselection is needed when the RC value reaches zero. Since vehicle communications are concerned with passenger safety, minimizing delay in resource selection and transmission latency is critical to avoid cases such as those investigated in [18]. Therefore, 3GPP proposed the maximum allowed latency not to exceed 100 ms (in this work, it is denoted by T_{step}) [Table A. 1.5-1 of [20]]. High channel load can prevent vehicles from transmitting CAM messages due to the maximum allowed latency. RC values are generated by each vehicle in three ranges $[5-15]$, $[10-30]$, and $[25-75]$, when T_{step} is equal to 100, 50 and 20 ms, respectively [7]. In this work, 100 ms T_{step} with $[5-15]$ RC range is proposed as the reselection parameter.

The number of resource blocks in each subchannel depends on the amount of data to be sent and the selected modulation and coding scheme (MCS). The number of sub-channels in one subframe of 1 ms is given by the following expression:

$$SCH_{sf} = \left\lfloor \frac{RB_{Tot}}{RB_{SCH}} \right\rfloor \tag{1}$$

where RB_{Tot} and RB_{SCH} are the total number of resource blocks in a given bandwidth and the number of resource blocks in a signal subchannel, respectively, while the symbol $\lfloor x \rfloor$ denotes the highest integer smaller than or equal to x. The total number of subchannels in T_{step} is denoted as $RES_{\max}$ and can be found as follows:

$$RES_{max} = SCH_{sf}\, T_{step} \tag{2}$$

The Channel Busy Ratio (CBR) is assumed in this work as a ratio of the used subchannels to the total number of subchannels in interval T_{step} as follows [22]:

$$CBR = \frac{S_{busy} + S_{sf}}{RES_{max}} \tag{3}$$

where S_{busy} and S_{sf} are the number of radio resources that experience a signal-to-interference plus noise ratio γ higher than the minimum allowed signal-to-interference plus noise

ratio $\gamma_{\min}$, and the number of all subchannels in the same subframe, respectively.

Furthermore, assume that the received power and the transmitted power are denoted P_r and P_t, respectively. Let the path loss exponent be denoted as α, and the path loss coefficient (on the linear scale) at the reference distance 1 m be PL_{loss}. The distance between the transmitter and the receiver is denoted by D. Then the received power can be written as follows:

$$P_r = \frac{P_t G_r}{PL_{loss} D^{\alpha}} \tag{4}$$

where G_r is the gain of the receiving antenna.

The distance D should be shorter than the maximum transmission range $D_{\max}$. Moreover, $D_{\max}$ is related to transmitted power, and $\gamma_{\min}$ by the following expression [22], [23]:

$$D_{\max} = \left[\frac{P_t G_r}{\gamma_{\min} PL_{loss} N_0} \right]^{\frac{1}{\alpha}} \tag{5}$$

where N_0 is the noise power in a subchannel. $\gamma_{\min}$ can be obtained by the following steps:

Step 1: Calculate the coding rate C_{rate} for the desired amount of data N_{Bits} [bits] as follows [23]:

$$C_{rate} = \frac{N_{Bits}}{2RB_{SCH} N_{symb} N_{SC} N_{el}} \tag{6}$$

where N_{symb}, N_{SC}, RB_{SCH} indicate the number of symbols that carry the desired data (equal to 9), the number of subcarriers in RB (equal to 12), and the number of resource blocks, respectively. The number of bits per symbol is indicated by N_{el}.

Step 2: Calculate the spectrum efficiency ζ [b/s/Hz]

$$\zeta = \frac{N_{Tot} N_{SC} N_{el} C_{rate}}{T_{Subf} RB_{band}} \tag{7}$$

where N_{Tot}, T_{Subf}, and RB_{band} are the total number of symbols in a subframe (equal to 14), the time duration of a sub-frame (equal to 1 ms), and the bandwidth of RB (equals 180 kHz), respectively.

Step 3: Calculate the minimum signal-to-interference-plus-noise ratio $\gamma_{\min}$ as

$$\gamma_{\min} = 2^{\frac{\zeta}{1-\Gamma}} - 1 \tag{8}$$

where Γ is the expected implementation loss, which is assumed to be 0.6 [24].

In this work, two modulation and coding schemes are applied; thus, two values of $\gamma_{\min}$ are calculated to obtain different $D_{\max}$ according to the transmission power for each of them.

III. SYSTEM MODEL

A. PROPOSED ALGORITHM

The proposed algorithm aims to generate multilevel *CBR* according to the concept of the DCC mechanism. The reaction of the system to the adjustment of *CBR* is represented by three factors at each level; maximum and minimum *CBR*, transmission power, and the established S-RSSI threshold. Moreover, the proposed channel load adjustment algorithm supports more flexible subchannel selection (with equal or lower than the maximum allowed schedule latency) by decreasing the number of vehicles in a vehicle transmission coverage range. This number of vehicles in a vehicle coverage range decreases by increasing the minimum threshold of SINR, which is equivalent to decreasing the receiving sensitivity and reducing the transmitted power based on CBR. In other words, the proposed algorithm increases or decreases channel utilization by tuning the minimum SINR threshold to the active levels of the DCC. The relaxed state is characterized by a minimum threshold for signal reception sensitivity that is represented by $S\text{-}RSSI_{thr,\min}$, maximum transmission power $P_{t,\max}$, and maximum acceptable CBR ($CBR_{\max,0}$). $CBR_{\max,0}$ is equal to the difference between unity and a specific fraction of CBR $\triangle CBR$ ($0 < \triangle CBR < 1$) set by the operator. The active state consists of N active levels ($n = 1, \ldots, N$). Each level n has a maximum and minimum CBR, transmission power $P_{t,n}$, and $S\text{-}RSSI_{thr,n}$. In the restrictive state, $S\text{-}RSSI$, it is proposed that the lowest limit of CBR reaches 0.1 of $CBR_{\max,0}$, while the transmission power reaches its lowest level.

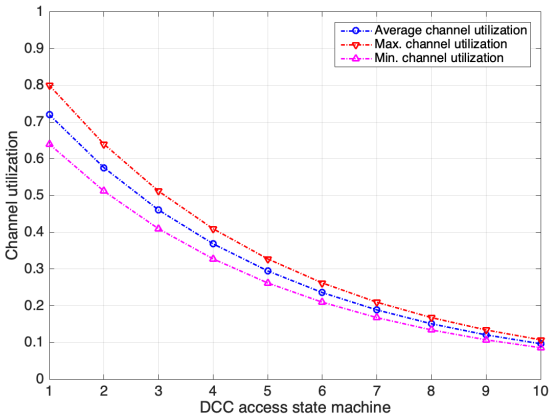

FIGURE 1. Example of change in channel utilization when applying the proposed algorithm through DCC access state machine.

The maximum CBR in the relaxed state can be expressed as follows.

$$A = 1 - \triangle CBR \tag{9}$$

$$CBR_{\max,0} = A \tag{10}$$

where A is the maximum CBR in the relaxed state. The maximum and minimum CBRs in the active state n are assumed to be given by the formulae:

$$CBR_{\max,n} = A^n \; CBR_{\max,0} \tag{11}$$

$$CBR_{\min,n} = A^{n+1} \; CBR_{\max,0} \tag{12}$$

According to the above equations, the value of CBR for a given level is in the range between the highest and lowest CBR of this level. These boundaries have the following

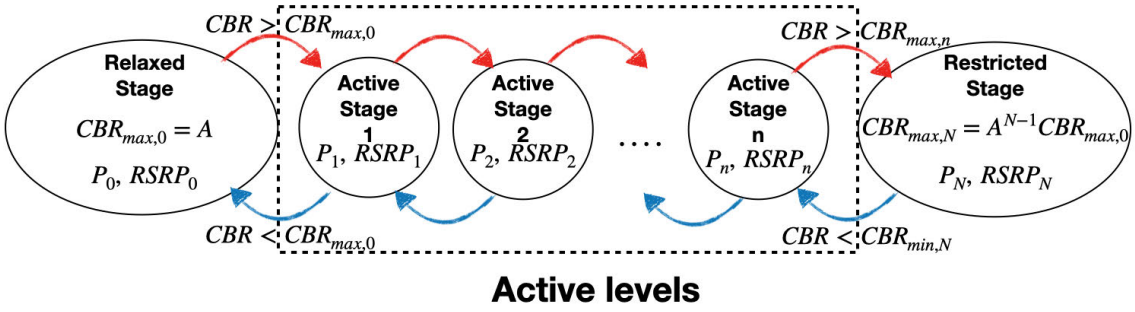

FIGURE 2. DCC access state machine with *n* active substates.

relationship with $CBR_{\max,0}$ of the relaxed state:

$$A^{n+1}CBR_{\max,0} \leq CBR_n < A^n CBR_{\max,0} \tag{13}$$

The maximum and minimum *CBR* that can be applied in the restrictive state can be found as follows.

$$CBR_{\max,N} = A^N \; CBR_{\max,0} \tag{14}$$

$$CBR_{\min,N} = A^{N+1} \; CBR_{\max,0} \tag{15}$$

According to (10) and (12), the number of levels of *CBR* is inversely proportional to the value of $\triangle CBR$ (that is, when the value of $\triangle CBR$ increases, the number of levels decreases).

As an example of changing channel utilization in DCC access stages, see Fig. 1. The relaxed and restricted stages are the first and last stages in the sequence of DCC access state machine, whereas the stages between them reflect the active levels for which channel utilization varies. However, channel utilization reduction leads to a user performance increase and spectral efficiency improvement.

The procedure of the proposed algorithm is presented in the form of a pseudocode in Algorithm 1.

In the algorithm input, n represents the current TPC-DCC level that a vehicle has used in the last T_{step} of the resource life cycle (when the RC reaches zero) before obtaining a new resource. CBR_{cur}, and $S\text{-}RSSI_{thr,n}$ are the current *CBR* and the threshold of *S-RSSI* at the level n. A vehicle obtains CBR_{cur} using (3), the subchannels are indicated as busy if *S-RSSI* is higher than $S\text{-}RSSI_{thr,n}$ of the current level. $S\text{-}RSSI_{thr,n}$ will continuously increase its threshold by 3 dB until it reaches the appropriate level of *CBR*. Furthermore, the number of increases also indicates the number of increases in levels. If the achieved number is greater than the number of levels, the next resource life cycle level will be the restrictive state. Furthermore, when CBR_{cur} is lower than the minimum *CBR* of this level, $S\text{-}RSSI_{thr,n}$ will continuously decrease its threshold by 3 dB until it achieves a *CBR* compatible with the current maximum and minimum *CBR*. Suppose the zero level is achieved, then the state machine achieves the relaxed state. The number of decreasing steps will also be the decreasing number of levels. According to the new level, a new transmission power $P_{t,n}$, the maximum and minimum *CBR* of the new level and a new $S\text{-}RSSI_{thr,n}$ will be established.

Algorithm 1 Proposed Adjusting Algorithm

Input: $n, N, CBR_{cur}, S\text{-}RSSI_{thr,n}, CBR_{\max,0}, A, RC$
Output: $CBR_{\max,n}, CBR_{\min,n}, P_t, S\text{-}RSSI_{thr,n}, RC$

while $RC = 0$ **do**
  if $CBR_{cur} > A^n \; CBR_{\max,0}$ **then**
    for i = 1 to N-n **do**
      $n = n + 1$
      $S\text{-}SRRI_{thr,n} = S\text{-}SRRI_{thr,n} + 3$ dB
      $CBR \leftarrow$ **Calculate a new CBR using (3)**
      if $CBR < A^n \; CBR_{\max,0}$ **then**
        break for loop
      end if
    end for
  else if $CBR_{cur} < A^{n+1} \; CBR_{\max,0}$ **then**
    for i = 1 to n **do**
      if $i \neq n$ **then**
        $S\text{-}SRRI_{thr,n} = S\text{-}SRRI_{thr,n} - 3$ dB
        $CBR \leftarrow$ **Calculate a new CBR using (3)**
        if $CBR > A^{n+1-i} CBR_{\max,0}$ **and** $CBR \leq A^{n-i} CBR_{\max,0}$ **then**
          $n \leftarrow n - i$
          break for loop
        end if
      else
        $n \leftarrow 0$
      end if
    end for
  end if
  $CBR_{\max,n} \leftarrow A^n \; CBR_{\max,0}$
  $CBR_{\min,n} \leftarrow A^{n+1} \; CBR_{\max,0}$
  $P_t \leftarrow P_{t,n}$ (P_t **assigned to level n (see Fig.2)**)
  $S\text{-}SRRI_{thr} \leftarrow S\text{-}SRRI_{thr,n}$
  $RC \leftarrow$ new RC
end while

B. SENSING-BASED SEMI-PERSISTENT SCHEDULING (S-SPS)

The status of the sensed resources in the physical layer should be constantly reported to the data link layer for analysis. When RC reaches zero in subframe t, the MAC layer will

ask the lower layer to send a report. This report should contain information on free resources in the period between $[t-1,(t-10T_{step})]$. The steps of S-SPS can be briefly summarized according to [7] as follows:

- The resources in the subframe that would serve the vehicle V_x are known as contiguous subchannels within the time interval $[t+T1, t+T2]$ where $T1$ can take any value lower than or equal to the time period of four subframes, depending on the processing time required for the selection operation. $T2$ is the maximum CAM interval $[20 \leq T2 \leq 100]$, depending on the maximum allowed latency.
- The vehicle V_x monitors all subframes in the time interval $[t-1,(t-10T_{step})]$.
- Vehicle V_x creates two lists: *ListA* that contains all resources that were sensed in the last time interval in the previous step, and *ListB* that is created as an empty list.
- In turn, V_x excludes all candidates that have Reference Signal Received Power (RSRP) greater than the established threshold.
- The remaining candidates should be greater than or equal to 20% of all candidates before excluding them. Otherwise, the previous step will be repeated with the established threshold of RSRP increased by 3 dB.
- The remaining candidates of *ListA* with the average Sidelink-Received Signal Strength Indicator (S-RSSI) of each subchannel given by equation (16) are moved to *ListB*.

$$S\text{-}RSSI_{avg} = \frac{1}{10}\sum_{i=1}^{10}\left[S\text{-}RSSI_{x,(t-i\cdot T_{step})}\right] \quad (16)$$

- *ListB* is reported to the higher layer. The MAC layer randomly picks up the next resource from *ListB*.

C. EXTENDED-ESTIMATION AND RESERVATION OF RESOURCE ALLOCATION (E-ERRA)

E-ERRA is an algorithm proposed in [10] and [11] by the authors of this article as an alternative scheduling algorithm to S-SPS to improve the reliability of the selection of free resources and to avoid packet collision in C-V2X Mode 4. As we have already mentioned, this algorithm uses extra information included in the SCI (about 2 bytes). It contains the RC of a broadcast packet, one bit that is set when the resource location is reserved by another vehicle in the network, the location of the collided resources in the awareness range, and the next resource location to use when the RC reaches zero. Depending on the decoded SCI of the received packet, the E-ERRA algorithm performs the following steps.

- The physical layer of V_x is continuously monitoring the subchannels of the last CAM interval $[t-1, t-T_{step}]$.
- *ListA* is initialized to collect all busy resources in the last CAM duration cycle T_{step}.
- *ListB* is initialized to collect all resources in the last CAM duration cycle.
- The vehicle V_x excludes all subchannel candidates from *ListA* that meet the following conditions:
  1) They have an RC value that is not equal to the RC of V_x.
  2) They have Reference Signal Received Power (RSRP) higher than the established threshold.
  3) They have been indicated as resources reserved by other vehicles in the awareness range ($b_{resv} \neq 0$), where b_{resv} is the bit indicating a location reserved by another vehicle.
  4) They have been indicated as a collided resource.
- *ListB* collects all resources that meet the following conditions:
  1) They are contained in subframes that have Reference Signal Received Power (RSRP) lower than the established threshold.
  2) They are contained in subchannels that have not been indicated as reserved resource locations by other vehicles ($b_{resv} \neq 0$).
- The remaining candidates for the resource locations in *ListA* should be placed in the First-In-First-Out (FIFO) queue with respect to receiving time. Furthermore, the remaining candidates in *ListB* should be arranged in the form of a resource location queue in ascending order with respect to the minimum S-RSSI.
- Vehicle V_x points the first resource location in *ListA* as the next reselection resource location in its SCI, when the RC reaches five. This way, vehicles in the surrounding area will know the location of the reserved resource. The vehicle that uses the reserved location will activate the reservation bit ($b_{resv} = 1$) at the next broadcast moment.
- Vehicle V_x continuously checks the availability of the reserved subchannel resource in the awareness range to ensure that it will be available when reselection is carried out. Otherwise, the first location of the resource in the *ListB* queue will be indicated as the next resource location of V_x.
- When the RC of V_x reaches zero, the reserved resource location is achieved and a new random RC value is generated for the new allocation of resources. The RC generator should exclude the RC values of the packets transmitted through subchannels located in the same subframe to avoid overlapping in future resource reselection.

IV. SIMULATION SCENARIOS AND ASSUMPTIONS

A. SYSTEM ASSUMPTIONS

A system layer simulation has been developed to test and compare the performance of the E-ERRA and S-SPS scheduling algorithms in interaction with the proposed multilevel adjustment of *CBR* in C-V2X Mode 4. The evaluation of the system model can be summarized in the following steps:

1) Each vehicle in the network evaluates the channel load at the last T_{step} of its resource life cycle before resource reselection.
2) Two separate simulations are run with two different MCSs for a constant inter-vehicle distance (the density

is constant over time) and for time-varying vehicle density.

3) The system is modeled to calculate the packet reception ratio and the resource collision ratio with both scheduling methods.
4) In (5), the maximum transmission distances are calculated for different transmission powers and the minimum signal-to-interference-plus-noise ratio is calculated for each MCS using (8).

It is important to note that the number of vehicles in the awareness range is calculated in each CAM period for each vehicle in the network.

B. SIMULATION SCENARIOS AND SETTINGS

Different highway scenarios have been designed using the Matlab platform. Matlab was integrated with the open source Simulation of Urban MObility (SUMO) package [34] to model more realistic environments. The scenarios of this work have been classified into two groups: standard network and hybrid network. Each of these groups consists of two scenarios. These scenarios differ in terms of vehicle distribution in the network, transmission power, and signal reception sensitivity as follows:

1) *Standard network*: The performance of the system layer has been investigated in a fixed inter-vehicle distance and service range. Furthermore, the number of vehicles in each lane of the highway is constant (wrapped network) during simulation time, as proposed in [33]. As mentioned above, the awareness range depends on the transmission power. Scenarios 1 and 2 have been simulated for different transmission powers and different MCSs; see Table 2.
2) *Hybrid network*: In these scenarios, the performance of the system layer has been investigated with varying vehicle densities (the distances between vehicles change over time). Thus, the transmission power will correspond to *CBR* of the resources in the service range of each vehicle. The service range can vary from one vehicle to another on the same network. The number of vehicles moving in each lane varies over simulation time. Furthermore, the transmission power should be related to the channel load in the service range according to the proposed multilevel adjustment of *CBR*. Scenarios 3 and 4 have been evaluated for different transmission powers and different MCS schemes, and are parameterized in Table 2. The purpose of these scenarios is to test the performance of the proposed congestion control algorithm in different vehicle densities in the same network and the interaction between the resource allocation methods and the proposed algorithm in more realistic environments.

In each simulation, the positions and distances of all vehicles in the network were updated and calculated in each CAM interval (assuming to be equal to 100 ms). Additionally, scheduling algorithms have been investigated and evaluated in all vehicles in the network for every CAM period.

TABLE 1. Common settings.

Common Parameters and settings	Values
Carrier frequency	5.9 GHz
Bandwidth	10 MHz
Shadowing	log-normal
Std. deviation	3
Road length × road width	2000 m × 4 m
No. of lanes in each direction	3
Frames duration	10 ms
Subframe duration	1 ms
Subcarrier space	15 KHz
No. of subcarriers in each RB	12
No. of symbols in sub-frame	14
No. of effective symbols in subframe	9
Vehicles speed in each direction	70, 100, 140 Kmph
Antenna gain G_r	3 dB
Path loss at 1 meter	20.06 dB
Loss exponent α	4
Noise power over 10 MHz	-95 dBm
CAM frequency f_b	10 Hz
CAM period T_{step}	100 ms
Packet size	190 bytes
Lowest RSRP	-92.5 dB
The maximum ratio difference $\triangle CBR$	0.2
The maximum CBR in the relaxed state	0.8

The common parameters for all scenarios are presented in Table 1. We assumed that the given channel bandwidth is 10 MHz. The Winner II B1 [33] propagation model was applied in our simulations. The maximum distances of the service ranges for specific transmission powers were calculated according to (5). Four highway scenarios were applied in several simulations that differed in selected parameters to obtain different results in the packet reception ratio and the packet collision ratio for different vehicle densities.

V. SYSTEM PERFORMANCE AND SIMULATION RESULTS

A. SYSTEM PERFORMANCE

In our simulations, we estimated two basic measures of packet transmission quality, namely, the Packet Reception Ratio *PRR* and the Collision Ratio *CR*. *PRR* is the ratio between the number of successfully decoded packets and the number of transmitted packets. *CR* is the ratio of packets that collided with other packets in the same coverage area to the total number of transmitted packets. *PRR* and *CR* have been calculated for all vehicles in the simulated network for each period of the CAM cycle for both resource scheduling algorithms in each scenario.

In order to be convinced that the simulation results obtained are sufficiently precise, we calculated the 95% confidence intervals for each estimated value applied in the figures showing PRR estimates. The width of each confidence interval $[x - \varepsilon, x + \varepsilon]$ depends on the estimated value x, but the relative value of the tolerance ε/x does not basically exceed 7% or is often lower. However, to ensure a clear view of the estimated plots, we decided not to show the confidence intervals in the figures.

B. SIMULATION RESULTS

This subsection shows the performance of the system layer for two scheduling algorithms with the proposed algorithm to

TABLE 2. Main scenarios, parameters and settings.

Parameters	Scenario 1	Scenario 2	Scenario 3	Scenario 4
Min-gap between vehicles for 70, 100, 140 km/h speed	12, 18, and 21 m	3, 7, and 10 m	variable	variable
No. of vehicles in the network	622	1375	See Fig.6	See Fig.7
The number of vehicles in the awareness range	constant	constant	variable	variable
PRB in one subchannel	12	6	12	6
Subchannels in one Subframe	4	8	4	8
Transmission power	16, 18, 20, and 22 dBm	24, 26, 28, and 30 dBm	16, 18, and 20	26, 28, 30 dBm
MSC Index	8	15	8	15
Coding rate C_{rate}	0.645	0.67	0.645	0.67
Min. SINR $\gamma_{\min}$	8.49 dB	18.76 dB	8.49 dB	18.76 dB
Max. Distances $D_{\max}$	503.7, 595.5, 704.1, and 832.5 m	513.9, 607.5, 718.3, and 849.30 m	503.7, 595.5, and 704.1 m	513.9, 607.5, 718.3, and 849.30 m
No. of simulations	8	8	2	2
Simulations time	5 sec.	6 sec.	6 sec.	5 sec.

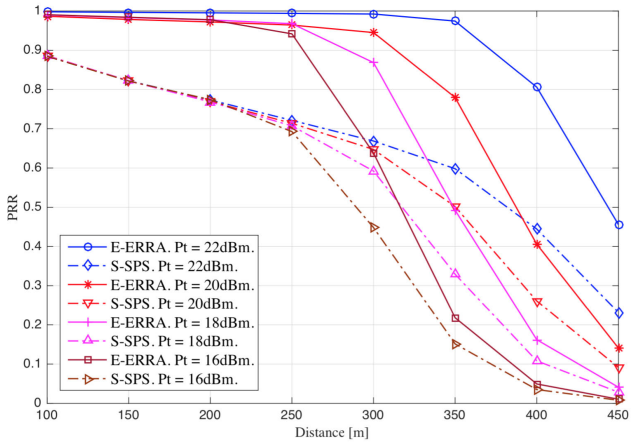

FIGURE 3. Performance comparison for E-ERRA and S-SPS algorithms in the form of *PRR* vs distance *D* in a standard network, in Scenario 1 with different broadcasting powers.

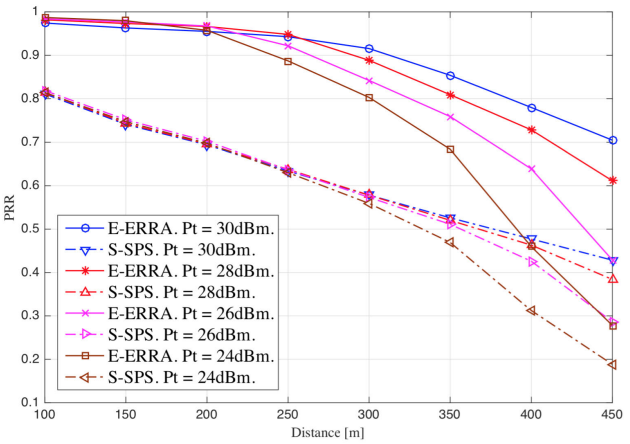

FIGURE 5. Performance comparison for E-ERRA and S-SPS algorithms in the form of *PRR* vs distance *D* in a standard network, in Scenario 2 with different broadcasting powers.

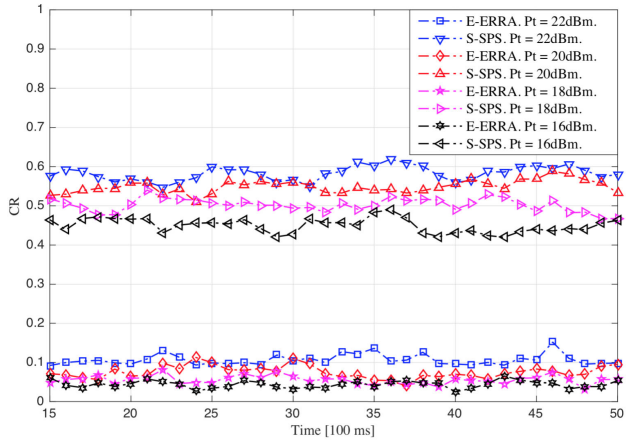

FIGURE 4. Performance comparison for E-ERRA and S-SPS algorithms in the form of packet Collision Ratio *CR* vs simulation time in a standard network with different broadcasting powers in Scenario 1.

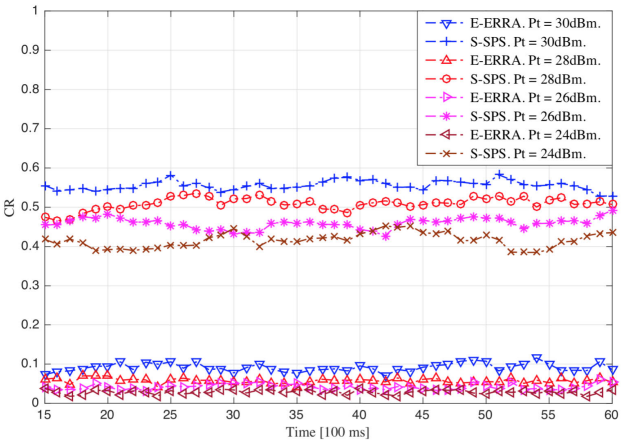

FIGURE 6. Performance comparison for E-ERRA and S-SPS algorithms in the form of packet Collision Ratio *CR* vs simulation time in a standard network with different broadcasting powers in Scenario 2.

adjust *CBR* levels. The E-ERRA and S-SPS scheduling algorithms have been tested, evaluated, and compared in two types of environments for two scenarios. The E-ERRA and S-SPS scheduling algorithms have been run with a combination

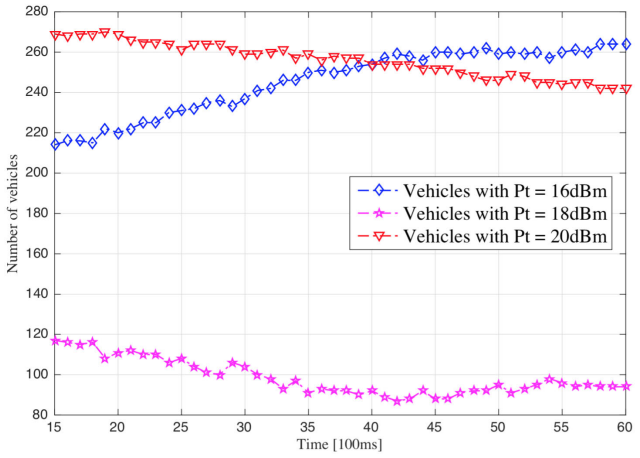

FIGURE 7. Variable number of vehicles in the network along simulation time in Scenario 3.

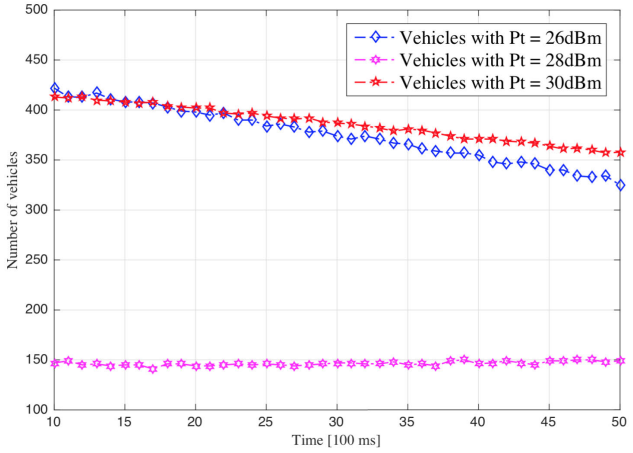

FIGURE 8. Variable number of vehicles in the network along simulation time in Scenario 4.

of TPC-DCC and adaptation of signal reception thresholds according to the calculation of the proposed levels. The performance of E-ERRA in terms of PRR in Fig. 3 for Scenario 1 (see Table 2) has shown promising results compared to S-SPS. *PRR* values increased from 11% over a distance of 100 m for all transmission powers to about 30-35% over 250 m and 2-20 % over 450 m for several transmission powers (see the legend in Fig. 3). In Scenario 2 (Fig. 5), the performance of *PRR* increases by about 18% for all transmission powers over a 100 m distance to 25-30% over 250 m, and to 11-30% in 450 m. The highest performance improvement for E-ERRA is observed when the highest transmission power is applied (in the relaxed state). Furthermore, high compatibility with the E-ERRA algorithm is observed when the proposed *CBR* levels are applied with the proposed adjustment method using TPC-DCC and adaptive sensitivity of reception signals. Increasing *CBR* levels provides greater precision in resource selection. However, Fig. 4 of Scenario 1 and Fig. 6 of Scenario 2 have shown an exceptionally significant improvement in the packet collision ratio *CR* when the E-ERRA algorithm is applied. The E-ERRA algorithm that uses reservation and tracking resources extremely reduces packet collisions. The results have shown a 50-60% improvement for E-ERRA compared to S-SPS in all transmission powers. It should be stressed that the E-ERRA algorithm has very high performance stability, high reliability in selecting resources, and low complexity in processing and implementation.

The numbers of vehicles in Scenarios 3 and 4 vary over time during the simulation time. The proposed methods to adjust the parameters have motivated us to avoid resource collision by continuously calculating *CBR* and selecting the appropriate level of parameters of the physical layer. Transmission power changes appropriately according to the channel load of vehicles in the transmission area. Thus, in the same network, there are different service ranges. Fig. 7 of Scenario 3 and Fig. 8 of Scenario 4, presented the variability of the number of vehicles in the network. These vehicles

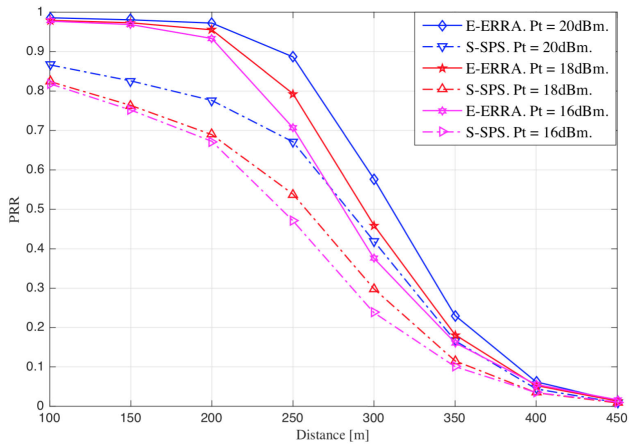

FIGURE 9. Performance comparison of E-ERRA and S-SPS algorithms in the form of *PRR* vs *Distance* in a hybrid network in Scenario 3 with different broadcasting powers.

broadcast packets with different transmission powers but apply the same MCS in each scenario.

Figs. 9 and 10 showed the *PRR* performance for vehicles that use different transmission power for broadcasting. Fig. 9 shows that the system performance of the E-ERRA algorithm is higher by about 13-18% than the performance of S-SPS.

The effect of limited resources and the impact of interference on these vehicles in the same network when using QPSK modulation (in Scenario 3) appeared strongly in the packet reception ratio compared to the standard network. Furthermore, the efficiency of the proposed method of adjusting physical parameters is limited by limited resources.

On the other hand, in Fig. 10, in 16QAM applications (Scenario 4), the resources have a higher level of channel load than in Scenario 3, and more flexibility is possible in the selection between these resources (the high number of resources provided more flexibility in the selection between several levels of the proposed *CBR* levels). Furthermore, these features were strongly supported by using

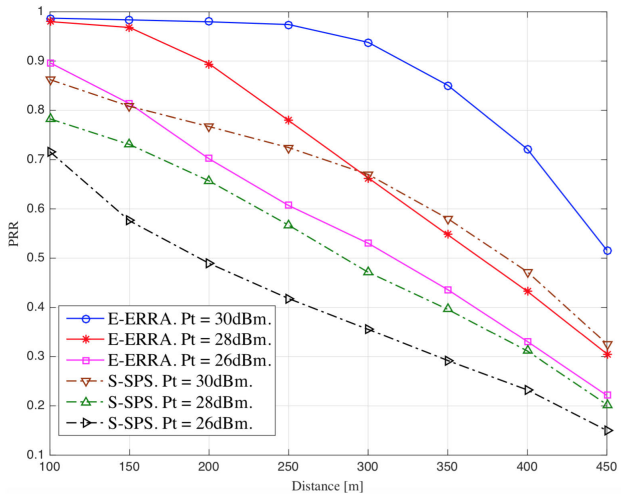

FIGURE 10. Performance comparison of E-ERRA and S-SPS algorithms in the form of *PRR* vs *Distance* in a hybrid network in Scenario 4 with different broadcasting powers.

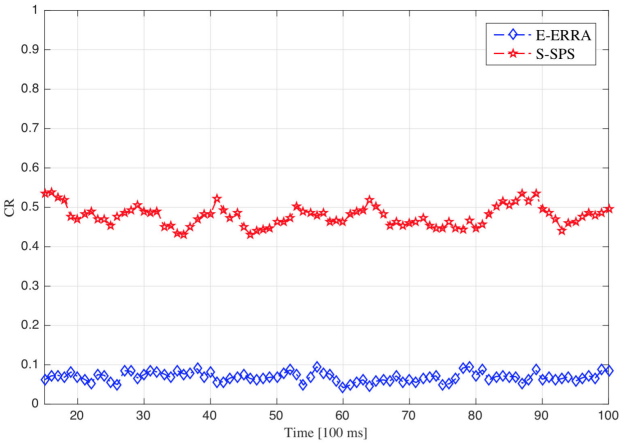

FIGURE 11. Collision Ratio *CR* vs simulation time in Scenario 3.

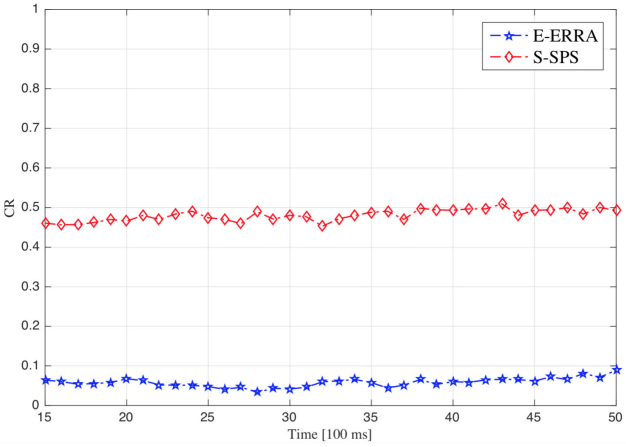

FIGURE 12. Collision Ratio *CR* vs simulation time in Scenario 4.

the *ListB* queue in the E-ERRA algorithm (Section II-C) to avoid resource selection collisions and compensate for losses in reserved resources that can appear when owners of the reserved resources have left the awareness range. In this scenario, E-ERRA has shown gradual enhancement compared to S-SPS by up to 27% when the distance is 300 m. The packet collision ratio in Figs. 11 and 12 in E-ERRA has shown about 40% higher efficiency compared to S-SPS by avoiding packet collision. Consequently, E-ERRA is more convenient than S-SPS broadcasting in the hybrid network environment. Increased levels of *CBR* with TPC-DCC and adaptive signal reception sensitivity show high compatibility with the E-ERRA algorithm compared to S-SPS.

VI. CONCLUSION

In this article, the DCC challenges for autonomous resource selection in V2X are investigated when channel load is high in the network. In this article, TPC-DCC and an adaptive power threshold of the received signal are engaged with a proposed algorithm of channel load adjustment based on the channel busy ratio in order to reduce the collisions in packets/resources and the interference effect. The E-ERRA and S-SPS resource allocation algorithms are considered for this purpose. The interactions of the proposed solutions with S-SPS and E-ERRA are investigated for fixed and flexible inter-vehicle distance environments. The simulation results for standard networks with E-ERRA supported by TPC-DCC have shown higher PRR, reliability in radio resource selection, and lower CR than S-SPS for all levels of physical parameters.

The E-ERRA algorithm is applied with TPC-DCC, adaptive signal sensitivity during reception, the proposed multi-level channel busy ratio algorithm in a hybrid network, and a variable number of vehicles in the same broadcast range. These network features have improved performance stability, PRR, and immunity against packet losses and CR compared to the case where the S-SPS algorithm is applied.

REFERENCES

[1] D. Jiang and L. Delgrossi, "IEEE 802.11p: Towards an international standard for wireless access in vehicular environments," in *Proc. VTC Spring IEEE Veh. Technol. Conf.*, Singapore, May 2008, pp. 1–6, doi: 10.1109/VETECS.2008.458.

[2] *Evolved Universal Terrestrial Radio Access (EUTRA) and Evolved Universal Terrestrial Radio Access Network (EUTRAN); Overall Description; Stage 2*, document 3GPP TS 36.300, Release 14, Version 14.0.0, Sep. 2016.

[3] *Study on Enhancement of 3GPP Support for 5G V2X Services*, document 3GPP TR 22.886, Release 15, Version 15.3.0, Sep. 2018.

[4] *Service Requirements for Enhanced V2X Scenarios*, document 3GPP TS 22.186, Release 16, Version 16.2.0, Jun. 2019.

[5] *Evolved Universal Terrestrial Radio Access (E-UTRA); Physical Channels and Modulation*, document 3GPP TS 36.211, Release 14 Version 14.4.0, Oct. 2017.

[6] N. Lyamin, A. Vinel, M. Jonsson, and B. Bellalta, "Cooperative Awareness in VANETs: On ETSI EN 302 637–2 performance," *IEEE Trans. Veh. Technol.*, vol. 67, no. 1, pp. 17–28, Jan. 2018, doi: 10.1109/TVT.2017.2754584.

[7] *Evolved Universal Terrestrial Radio Access (E-UTRA); Physical Layer Procedures*, document 3GPP TS 36.213, Release 14, Version 14.4.0, Oct. 2017.

[8] *Intelligent Transport Systems (ITS) Vehicular Communications; Basic Set of Applications; Part 2: Specification of Cooperative Awareness Basic Service*, Standard EN 302 637-2, Version 1.3.2, ETSI, Apr. 2019.

[9] *Evolved Universal Terrestrial Radio Access (E-UTRA); Multiplexing and Channel Coding*, document 3GPP TS 136.212, Release 15, Version 15.2.1, Jul. 2018.
[10] S. Sabeeh, P. Sroka, and K. Wesolowski, "Estimation and reservation for autonomous resource selection in C-V2X mode 4," in *Proc. IEEE 30th Annu. Int. Symp. Pers., Indoor Mobile Radio Commun. (PIMRC)*, İstanbul, Turkey, Sep. 2019, pp. 1–6.
[11] S. Sabeeh and K. Wesolowski, "C-V2X mode 4 resource allocation in high mobility vehicle communication," in *Proc. IEEE 31st Annu. Int. Symp. Pers., Indoor Mobile Radio Commun. (PIMRC)*, London, U.K., Aug. 2020, pp. 1–6.
[12] *Intelligent Transport Systems (ITS); Decentralized Congestion Control Mechanisms for Intelligent Transport Systems Operating in the 5 GHz Range; Access Layer Part*, Standard ETSI TS 102 687, Version 1.2.1, Apr. 2018.
[13] *Intelligent Transport Systems (ITS); Congestion Control Mechanisms for the C-V2X PC5 Interface; Access Layer Part*, Standard ETSI TS 103.574, Version 1.1.1, Nov. 2018.
[14] M. Yu, A. Malvankar, and W. Su, "A distributed radio channel allocation scheme for WLANs with multiple data rates," *IEEE Trans. Commun.*, vol. 56, no. 3, pp. 454–465, Mar. 2008.
[15] J. Ng and M. Yu, "A new model for the efficient channel utilization of wireless networks and applications," in *Proc. IEEE Wireless Commun. Netw. Conf. Workshops (WCNCW)*, Mar. 2015, pp. 176–181, doi: 10.1109/WCNCW.2015.7122550.
[16] A. Mansouri, V. Martinez, and J. Harri, "A first investigation of congestion control for LTE-V2X mode 4," in *Proc. 15th Annu. Conf. Wireless On-Demand Netw. Syst. Services (WONS)*, Wengen, Switzerland, Jan. 2019, pp. 56–63, doi: 10.23919/WONS.2019.8795500.
[17] M. Sepulcre, J. Mira, G. Thandavarayan, and J. Gozalvez, "Is packet dropping a suitable congestion control mechanism for vehicular networks?" in *Proc. IEEE 91st Veh. Techn. Conf. (VTC-Spring)*, Antwerp, Belgium, May 2020, pp. 1–5, doi: 10.1109/VTC2020-Spring48590.2020.9128822.
[18] S. Sabeeh, "Centralized resource allocation latency of SideLink communication in NR V2X," in *Proc. IEEE 96th Veh. Technol. Conf. (VTC-Fall)*, London, U.K., Sep. 2022, pp. 1–6.
[19] B. McCarthy and A. O'Driscoll, "Congestion control in the cellular-V2X sidelink," 2021, *arXiv:2106.04871*.
[20] *Technical Specification Group Radio Access Network; Study on LTE-Based V2X Services*, document 3GPP TS 36.885, Release 14, Version 14.0.0, Jun. 2016.
[21] A. Bazzi, G. Cecchini, B. M. Masini, and A. Zanella, "Should I really care of that CAM?" in *Proc. IEEE 29th Annu. Int. Symp. Pers., Indoor Mobile Radio Commun. (PIMRC)*, Bologna, Italy, Sep. 2018, pp. 1–6.
[22] S. Sabeeh and K. Wesolowski, "Resource re-selection with adaptive modulation and collision detection in LTE V2X mode 4," in *Proc. IEEE 32nd Annu. Int. Symp. Pers., Indoor Mobile Radio Commun. (PIMRC)*, Sep. 2021, pp. 1005–1010, doi: 10.1109/PIMRC50174.2021.9569449.
[23] S. Sabeeh, K. Wesołowski, and P. Sroka, "C-V2X centralized resource allocation with spectrum re-partitioning in highway scenario," *Electronics*, vol. 11, no. 2, p. 279, Jan. 2022.
[24] *Evolved Universal Terrestrial Radio Access (E-UTRA); Radio Frequency (RF) System Scenarios*, document 3GPP TR 36.942, Version 14.0.0, Mar. 2017.
[25] S. Chen, J. Hu, Y. Shi, Y. Peng, J. Fang, R. Zhao, and L. Zhao, "Vehicle-to-everything (V2X) services supported by LTE-based systems and 5G," *IEEE Commun. Standards Mag.*, vol. 1, no. 2, pp. 70–76, 2017.
[26] A. Bazzi, B. M. Masini, A. Zanella, and I. Thibault, "Beaconing from connected vehicles: IEEE 802.11p vs. LTE-V2V," in *Proc. IEEE 27th Annu. Int. Symp. Pers., Indoor, Mobile Radio Commun. (PIMRC)*, Sep. 2016, pp. 1–6.
[27] M. Wang, M. Winbjork, Z. Zhang, R. Blasco, H. Do, S. Sorrentino, M. Belleschi, and Y. Zang, "Comparison of LTE and DSRC-based connectivity for intelligent transportation systems," in *Proc. IEEE 85th Veh. Technol. Conf. (VTC Spring)*, Sydney, NSW, Australia, Jun. 2017, pp. 1–5.
[28] D. Smely, S. Rührup, R. Schmidt, J. Kenney, and K. Sjöberg, "Decentralized congestion control techniques for VANETs," in *Vehicular Ad Hoc Networks: Standards, Solutions and Research*, C. Campolo, A. Molinaro, and R. Scopigno, Eds. Berlin, Germany: Springer, 2015.
[29] S. Ucar, S. C. Ergen, and O. Ozkasap, "Multihop-cluster-based IEEE 802.11p and LTE hybrid architecture for VANET safety message dissemination," *IEEE Trans. Veh. Technol.*, vol. 65, no. 4, pp. 2621–2636, Apr. 2016.
[30] M. Gonzalez-Martín, M. Sepulcre, R. Molina-Masegosa, and J. Gozalvez, "Analytical models of the performance of C-V2X Mode 4 vehicular communications," *IEEE Trans. Veh. Technol.*, vol. 68, no. 2, pp. 1155–1166, Feb. 2018.
[31] M. H. C. Garcia, A. Molina-Galan, M. Boban, J. Gozalvez, B. Coll-Perales, T. Sahin, and A. Kousaridas, "A tutorial on 5G NR V2X communications," *IEEE Commun. Surveys Tuts.*, vol. 23, no. 3, pp. 1972–2026, 3rd Quart., 2021, doi: 10.1109/COMST.2021.3057017.
[32] A. Bazzi, B. M. Masini, A. Zanella, and I. Thibault, "On the performance of IEEE 802.11p and LTE-V2V for the cooperative awareness of connected vehicles," *IEEE Trans. Veh. Technol.*, vol. 66, no. 11, pp. 10419–10432, Nov. 2017.
[33] P. Kyösti, J. Meinilä, L. Hentilä, X. Zhao, T. Jämsä, C. Schneider, M. Narandzić, M. Milojević, A. Hong, J. Ylitalo, V.-M. Holappa, M. Alatossava, R. Bultitude, Y. de Jong, and T. Rautiainen, "IST-4-027756 WINNER II, deliverable D1.1.2 V1.2 channel models," EBITG, TUI, UOULU, CU/CRC, Nokia, Tech. Rep., 2007.
[34] D. Krajzewicz, G. Hertkorn, C. Rössel, and P. Wagner, "SUMO (simulation of urban mobility)—An open-source traffic simulation," in *Proc. 4th Middle East Symp. Simulation Modeling (MESM)*, Dubai, United Arab Emirates, Sep. 2002, pp. 183–187.

SAIF SABEEH (Member, IEEE) was born in Baghdad, Iraq. He received the M.S. degree in electronics and telecommunication engineering from the Poznan University of Technology (PUT), Poznan, Poland, in 2017, where he is currently pursuing the Ph.D. degree in information and communication technologies. His research interests include radio resource allocation in 5G and beyond technologies, vehicle-to-everything (V2X) communication, device-to-device (D2D) communication, space-time block coding, MIMO technology, and mmWave propagation channel design.

KRZYSZTOF WESOŁOWSKI (Life Member, IEEE) received the Ph.D. and Dr. habil. degrees in communications from the Poznan University of Technology (PUT), in 1982 and 1989, respectively.

He was the Dean of the Faculty of Electronics and Telecommunications at PUT. He was a Postdoctoral Fulbright Scholar at Northeastern University, Boston, and a Postdoctoral Alexander von Humboldt Scholar at the University of Kaiserslautern, Germany. He also worked at the University of Kaiserslautern as a Visiting Professor. He has been employed with PUT, since 1976. Since 1999, he has been a Full Professor of telecommunications. He is the author or coauthor of more than 150 scientific publications, including the books: *Mobile Communication Systems* (John Wiley & Sons, Chichester, 2003) and *Introduction to Digital Communication Systems* (John Wiley & Sons, Chichester, 2009). He published his results, among others, in IEEE Transactions on Communications, IEEE Journal on Selected Areas in Communications, IEEE Transactions on Vehicular Technology, *IEE Proceedings*, *European Transactions on Telecommunications*, *Electronics Letters*, and *EURASIP Journal on Wireless Communications and Networking*. His team participated in several domestic and international research projects funded by industry and the European Union within the Sixth and Seventh Framework Programs. In his scientific activity, he specializes in digital wireline and wireless communication systems, information and coding theory, and DSP applications in digital communications.